Synthesis and characterization of a redox-active ion channel supporting cation flux in lipid bilayers

Maia Tsikolia,*[b] Adam C. Hall,[a] Cristina Suarez,[a] Zazi O. Nylander,[a] Sarah M. Wardlaw,[a] Molly E. Gibson,[a] Kerry L. Valentine,[a] Louisa N. Onyewadume,[a] Deborah A. Ahove,[a] Maya Woodbury,[a] Margaret M. Mongare,[a] C. Dennis Hall,[b] Zuoquan Wang,[b] Bogdan Draghici[b] and Alan R. Katritzky[b]

Received 14th April 2009, Accepted 10th June 2009
First published as an Advance Article on the web 22nd July 2009
DOI: 10.1039/b907350g

The synthesis, cation binding and transmembrane conductive properties of a novel synthetic ion channel containing a redox-active ferrocene unit are described. Fluorescence spectroscopy was used to demonstrate that the channel supports multiple ion coordination and association constants for 1:1 and 1:2 (channel:cation) coordination for both Na^+ and K^+ were evaluated. Experiments using a black lipid membrane preparation revealed that this compound functioned effectively as an ion channel for both Na^+ and K^+. Concomitant ^{23}Na NMR spectroscopy studies supported this finding and revealed a Na^+ flux, at least 5 times higher than ion transport rates by monensin. Furthermore, oxidation of the redox-active centre (Fe^{2+} to Fe^{3+}) effectively inhibited ion transport.

Introduction

The passage of ions and other materials across cellular membranes is a crucial biological process and hence extensive research has been devoted to understanding mechanisms of ion transport.[1,2] During the last two decades, efforts have been made to mimic the action of biological ion channels by the synthesis of model systems that span lipid bilayers.[3] Synthetic proteins have been designed to mimic natural channels, albeit with a single span rather than the multiple transmembrane domains typical of biological systems.[4] Other designs include self-assembling cyclic peptide nanotubes[5] that have been shown to be toxic to bacteria by introducing a pore through the plasma membrane[5c] and metal-organic frameworks[6] which may offer a new dimension to synthetic ion channels. During the last decade selective artificial channels have been fashioned with head groups (*e.g.* macrocyclic polyethers or carbonyl groups) to capture specific ions, long aliphatic chains designed to span the bilayer and 'relay units', such as other macrocyclic ethers, to shuttle ions across the membrane.[7–12] The 'relay unit' is seen as a potential means of stabilizing cations through hydration by hydrogen-bonded water[13] or coordination with carbonyl functions.[9] This multiple ion transport, known as the 'billiard ball effect' (in essence, the charge repulsion theory of multiple ion transport[14]) has been corroborated in channels using other head groups such as the calixarenes.[15] Electrospray mass spectrometry has served to enhance this view of multiple ion complexation in some artificial channels.[16]

In the following study we describe a novel synthetic ion channel containing a ferrocene unit (**9**, Scheme 1). As in previous work[17] fluorescence spectroscopy was used to study qualitative and quantitative aspects of cation binding, by inhibition of photoelectron transfer from tricoordinate nitrogen to the photoexcited state of pendant 9-methylanthryl groups. The fluorophores also served to 'anchor' the channel in phospholipid bilayers.

Two techniques were used to characterize conductance across bilayers mediated by **9**. Ion channel activity was first assessed using ^2Na NMR spectroscopy in order to measure cumulative rates of cation transport across a vesicle membrane.[18–20] This method relies on monitoring the rate of exchange of the cation between the intra- and extra-vesicular environments where the chemical shift of the extra-vesicular cation is subject to a chemical shift reagent (*e.g.* Dy^{3+}). This technique has been widely exploited, especially by Gokel *et al.*,[13] to examine rates of cation transport across membranes infused with artificial channels. The impact of oxidation of **9** on its potential as a conducting ion channel was also determined using the same methodology. The second method employed the black lipid membrane technique to record single (or multiple) open channel events evoked by the artificial ion channel, enabling calculations of single channel conductance and current–voltage relationships for the ion channel activity.

The artificial channel used in this study was designed with four specific features in mind:

(i) the channel length was 35–40 Å in an attempt to mimic the dimensions of biological channels;

(ii) the terminal nitrogen atoms were equipped with 9-methylanthryl groups to afford fluorescence detection of cation coordination and to function as hydrophobic anchors within a lipid membrane;

(iii) the central macrocyclic rings were derived from diaza-15-crown-5 in an attempt to achieve selectivity between Na^+ and K^+;

(iv) the central unit contained ferrocene to act as a redox centre (and therefore a potential switch) and to provide rigidity within the channel structure.

[a]*Program in Biochemistry, Dept. Biological Sciences, Smith College, Northampton, MA 01063, USA. E-mail: ahall@science.smith.edu; Fax: 413-585-3786; Tel: 413-585-3467*
[b]*Center for Heterocyclic Compounds, Department of Chemistry, 126 Sisler Hall, University of Florida, Gainesville, FL 32611-7200, USA. E-mail: cdennishall@aol.com; Fax: 352-392-9199; Tel: 352-392-0554*

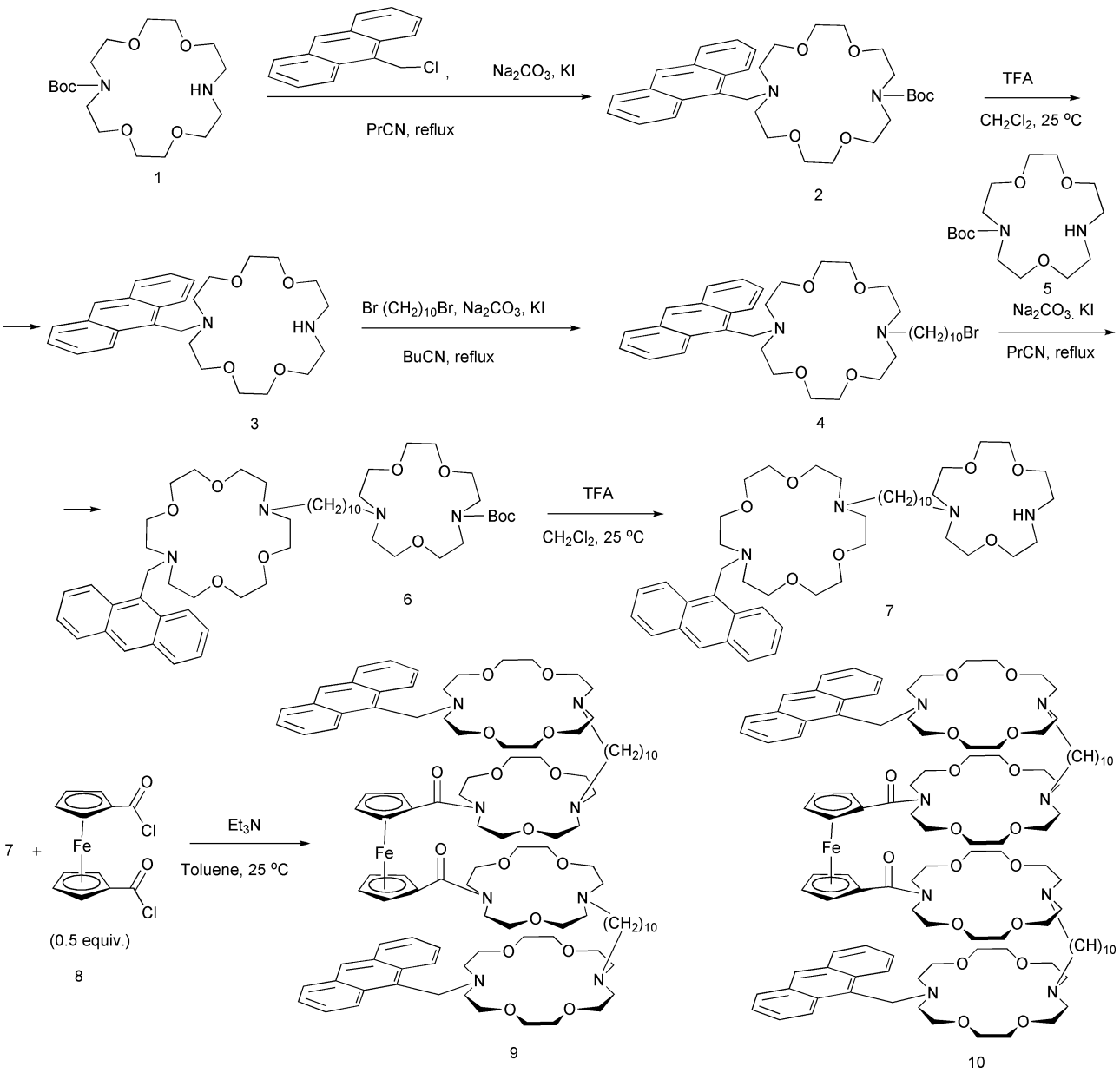

Scheme 1

Results and discussion

1. Synthesis of redox-active ion channels

The ion channel **9** chosen for this particular study was synthesized by condensation of mono-N-Boc-diaza-18-crown-6 (**1**) with 9-chloromethylanthracene, removal of the protecting group from **2**, condensation of the product **3** with 1,10-dibromodecane (1:1 molar ratio), condensation of the product **4** with mono-N-Boc-diaza-15-crown-5 (**5**)[21], deprotection of the bicyclic product **6** and condensation of two moles of the resultant amine **7** with 1,1′-ferrocenyl diacid chloride (**8**) (Scheme 1). The compounds were characterized by high resolution mass spectrometry and $^{1}H/^{13}C$ NMR (see Experimental).

2. Cation binding by fluorescence spectroscopy

The 9-anthrylmethyl groups of the channel serve as fluorescent tags for the detection and possible quantification of coordination with cations. Fluorescence in the uncomplexed channel is suppressed by photoelectron transfer (PET) from tricoordinate nitrogen within the diazamacrocycles. Coordination with cations suppresses PET and results in various degrees of enhanced fluorescence dependent on the charge density and association constants of the cations involved.[22] In qualitative terms this is reflected in the fluorescence intensities recorded at 411 nm (λ_{exc} = 363 nm) with a cation : ion channel ratio of 50:1, which were shown to decrease in the following order, $Mg^{2+} > Ca^{2+} > Na^{+} > K^{+}$ (Fig. 1 for Na^{+} and K^{+} only).

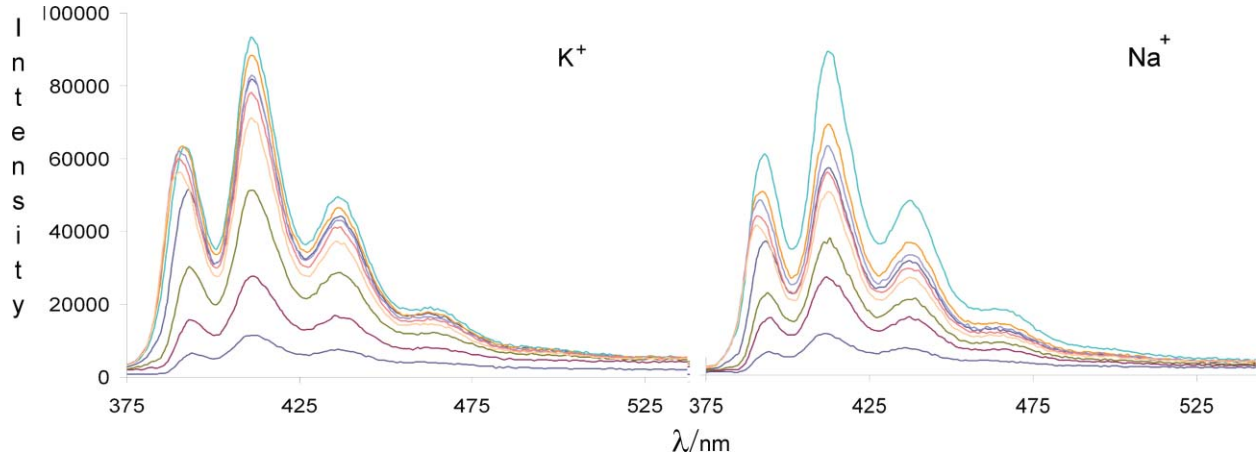

Fig. 1 Fluorescence emission intensity of **9** (10^{-4} M) as a function of added KSO_3CF_3, $NaSO_3CF_3$ (0.1M) in CH_3CN (25 °C, λ_{exc} = 363 nm). Intensity increasing with molar ratio (**9** : M^+) increasing from 1:0 to 1:50.

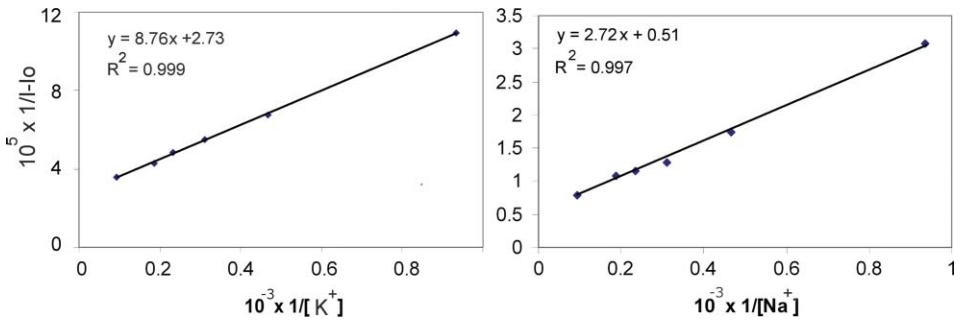

Fig. 2 Plots of $1/I - Io$ *vs* $1/M^+$ for K^+ and Na^+ at 2×10^{-5} M of **9**.

The quantitative aspects of cation coordination as determined by fluorescence spectroscopy are dependent on the initial concentration of the channel. At *ca.* 10^{-5} M in ion channel, increasing concentrations of cation from 5×10^{-5} to 2×10^{-4} M gave fluorescence intensities (I – Io) that fitted a 1:1 coordination ratio (eqn 1) to give association constant (K_1) values of *ca.* 33,000 and *ca.* 19,000 for K^+ and Na^+ respectively (Fig. 2). A similar plot using Ca^{2+} gave a K_1 value of 106,000 reflecting association of an ion with a similar ionic radius to that of sodium but a much greater charge density.

$$1/(I - Io) = 1/K\Delta\varepsilon[IC_0][M^+] + 1/\Delta\varepsilon[IC_0] \quad (1)$$

Where I = fluorescence intensity; K = 1:1 association constant; $\Delta\varepsilon$ = difference in fluorescence intensity extinction coefficient between ion channel and complex; $[IC_0]$ = ion channel initial concentration and $[M^+]$ = concentration of cation. The association constants were obtained by a plot of $1/(I - Io)$ *vs* $1/[M^+]$ which, for 1:1 stoichiometry is linear with slope, $S = 1/K\Delta\varepsilon[IC_0]$ and intercept, $I = 1/\Delta\varepsilon[IC_0]$; thus $K = I/S$.

The higher K_1 value for K^+ over Na^+ is consistent with coordination by an 18-C-6 system favouring K^+ over Na^+[23] and suggests that the initial coordination involves the outside 18-C-6 rings. As the concentration ratio exceeds 10:1 (M^+ : ion channel) values of I – Io show an increase over the 1:1 complex maximum indicating the development of a higher degree of coordination. At 2×10^{-4} M in ion channel, Job plots using 0.1 M solutions of K^+ and Na^+ cations reveal a clear 2:1 cation : ion channel ratio (Fig. 3).

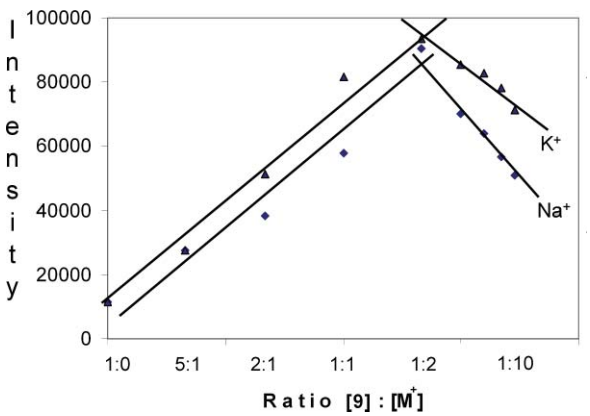

Fig. 3 Job plots using 0.1 M solutions of K^+ (▲) and Na^+ (◆) cations at 2×10^{-4} M of **9**.

At 2×10^{-4} M and a K_1 value of 33,000 the 1:1 complex is formed to the extent of at least 70%. Beyond 4×10^{-2} M in cation the 1:1 complex is >90% formed and any further increase in I – Io values is associated with 2:1 cation : ion channel complex formation. Thus quantitative aspects of coordination at higher ion channel concentration were evaluated for K^+ and Na^+ by assuming that the 1:1 complexes were essentially fully formed before treating the subsequent data again using eqn. 1 (Fig. 4).

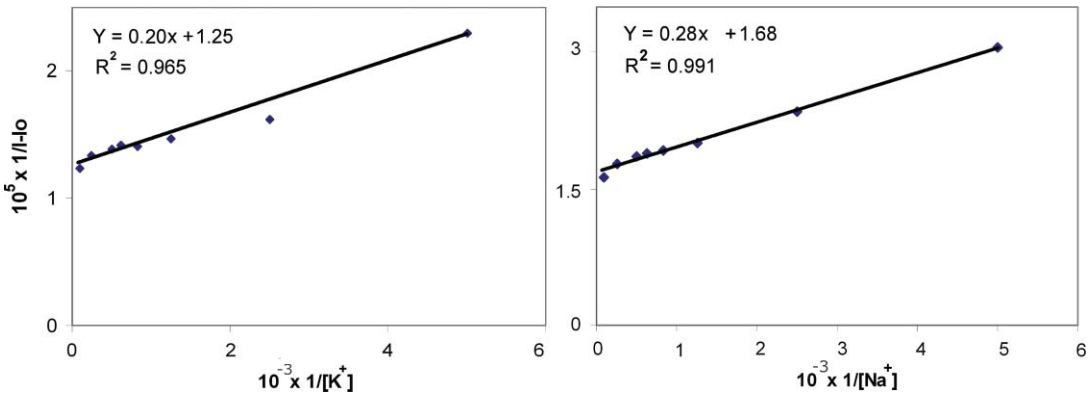

Fig. 4 Plots of 1/I – Io *vs* $1/M^+$ for K^+ and Na^+ at 2×10^{-4} M of **9**.

The results for K^+ and Na^+ are K_2 values of 11,000 and 6,500 respectively, approximately three times lower than the corresponding K_1 values. This is entirely consistent with coordination of a second cation responding to cation repulsion, a concept that complements the so-called "billiard ball effect" as an essential feature of ion channel activity.[14] Beyond 20:1 cation : ion channel at 2×10^{-4} M in ion channel, a further increase in I – Io was observed indicating a 3:1 (or possibly ultimately a 4:1) coordination ratio. This is consistent with ^{13}C NMR and cyclic voltammetry data reported for the analogous ion channel[17] (**10**, Scheme 1).

In conclusion the fluorescence studies reveal coordination with alkali and alkaline earth cations and in the case of Na^+ and K^+ multiple complexation of each cation with the ion channel is observed as expected for a system with four macrocyclic rings.

3. Cation transport by ^{23}Na NMR spectroscopy

The ion channel cation flux of **9** across unilamellar vesicles was assessed using ^{23}Na NMR spectroscopy. Our previous study[17] showed that a linewidth broadening of the Na^+_{IN} ^{23}Na NMR signal could be used to monitor sodium transport across lipid bilayers. We set out to use a similar methodology to measure and afterwards compare the cation flux properties of both synthetic ion channels. Unilamellar vesicles were prepared by the dialytic detergent removal technique following the protocol outlined in the Experimental section. This method is reported to give a spread of vesicle diameters between 200 and 600 nm. Encapsulation of intravesicular sodium was found to be consistent with previous preparations as shown by a consistent integration of the Na^+_{IN} NMR signal of ~12% of total sodium available. NMR samples were prepared in 5 mm NMR tubes using a small volume of vesicle suspension (0.75 ml) that was treated with 3 μl of a 1 M aqueous solution of the shift reagent $DyCl_3$ and 75 μl of D_2O. Dysprosium induces a separation of the Na^+_{IN} and Na^+_{OUT} NMR signals by shifting the extravesicular sodium (Na^+_{OUT}) signal ~6–10 ppm upfield. Once separation was confirmed and the system equilibrated (<5 min), known microliter amounts of 5 mM **9** were added and the resultant broadening of the Na^+_{IN} signal was monitored over time.

Four different microliter amounts (1 μl, 2 μl, 3 μl and 5 μl) of the 5 mM solution of **9** were introduced into separate vesicular suspensions, resulting in concentrations of **9** at 6.6, 13.2, 19.8 and 33.0 μM respectively. Fig. 5 shows an experiment in which

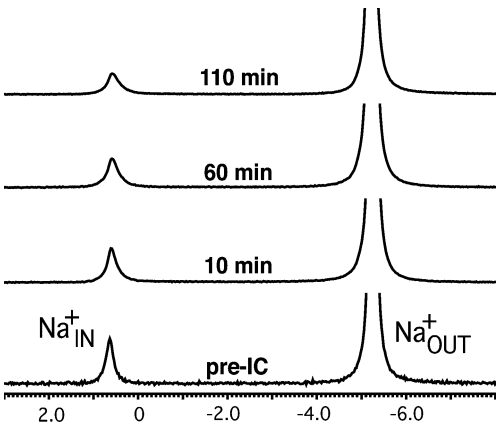

Fig. 5 ^{23}Na NMR spectra of a single vesicular suspension containing 3.0 μl of 1 M $DyCl_3$. NMR spectra taken prior to, and at different times (10, 60 and 110 minutes) after the addition of **9** (13.2 μM) at 297 K.

the change in NMR signal linewidth was monitored with respect to time after the addition of 13.2 μM **9**. The broadening of the Na^+_{IN} NMR signal in the presence of **9** can be quantitatively measured with respect to time, reaching equilibrium conditions after approximately 2 h. Fig. 6 shows the plot obtained from the linewidth broadening at half height (ΔLW) *versus* time for two separate 13.2 μM and 19.8 μM additions of **9** to vesicular

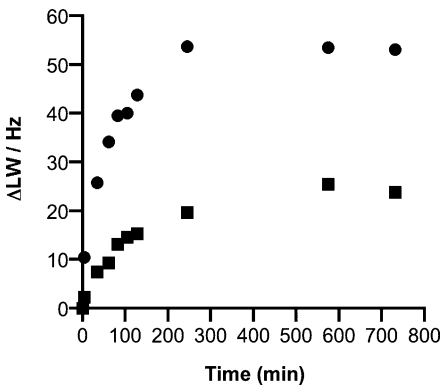

Fig. 6 Sample time dependence of the linewidth broadening (ΔLW) of the Na^+_{IN} NMR signal on addition of 13.2 μM (■) and 19.8 μM (●) of **9** to separate standard vesicle preparations.

Table 1 Observed linewidths (LW) in Hz of the Na^+_{IN} peak *vs* [**9**] together with the corresponding rate constants (k_{obs}) for Na^+ exchange

[**9**] × 10^6/M	Time/min	LW(Na^+_{IN})	LW(Na^+_{OUT})	k_{obs}/s^{-1} [a]
	0	24	17	
6.6	4	27	17	
6.6	120	28	18	13.1
	0	22	18	
13.2	5	26	16	
13.2	120	36	18	41.2
	0	19	16	
19.8	5	29	17	
19.8	213	42	18	53.2
	0	26	20	
33.0	5	36	19	
33.0	120	82	20	169.6

[a] Normalized to the linewidth of the Na^+_{OUT} linewidth. In the case of [**9**] = 13.2×10^{-6} M and [9] = 19.8×10^{-6} M the average LW(Na^+) of multiple runs was evaluated.

suspensions. As expected, the change in linewidth broadening was markedly larger for the 19.8 μM *versus* the 13.8 μM addition.

As seen previously[17] with **10**, the NMR signal broadening behaviour is indicative of cation transport and its characterization yields kinetic information. The broadening also confirms that the smaller ring size of the inner aza crown-ether macrocycles in **9** in comparison with **10** does not preclude sodium transport. Table 1 shows the resultant linewidths and calculated rate constants ($k_{obs} = \pi \times \Delta LW$) for sodium transport *via* **9** for all given concentrations.

A plot of k_{obs} *vs* [**9**] was linear (Fig. 7) yielding a k_2 value of 5×10^6 l mol^{-1} s^{-1}, which indicates relatively rapid bulk sodium transport, at least five times faster than the rate of transport measured with monensin, a well-characterized ion transporter.[19a]

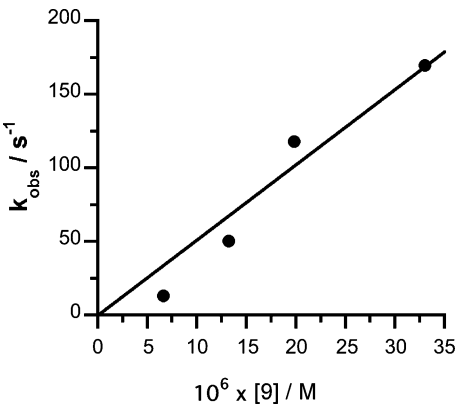

Fig. 7 Plot showing the linear relationship between k_{obs} and [**9**] yielding a k_2 value of 5.1×10^6 l mol^{-1} s^{-1}.

This k_2 value is similar to that obtained for sodium transport under the same LUV conditions ([Na^+] = 200 mM) using our previous synthetic ion channel **10**, which exhibited $k_2 = 6 \times 10^6$ l mol^{-1} s^{-1}. This indicates that the smaller ring size of the inner aza crown-ether macrocycle in **9** does not interfere with the overall transport of, at least, sodium. It is noteworthy that we observed a substantial variability in rates between NMR trials using **9** that was not observed for **10**, and the figures reported are averages. In the literature, transport rate variability has been observed with other synthetic ion transporters. Elliott and co-workers studying amphiphilic synthetic ionophores pointed out the presence in some of an aggregation state pre-incorporation, which had an effect ultimately on ion release kinetics.[24] As in our case, the addition of the synthetic ion channel as an organic solution to the aqueous suspension of the vesicles might have enhanced the formation of aggregates manifesting itself in the variability of the NMR transport studies.

Finally an interesting feature of **9**, as it was of **10**, was the inclusion of a ferrocene redox-active centre to act as a device for the regulation of ion flux. We followed the same protocol designed to test the potential gating ability of the redox centre in **9** as for **10**. A fresh sample of vesicles and ion channel were mixed and monitored for Na^+_{IN} NMR lineshape broadening. The presence of sodium transport was established and recorded. Then a separate aqueous solution of **9** was prepared (5 mM) and treated with an equimolar amount of cerium (IV) ammonium nitrate. Immediate addition of the treated ion channel to a fresh sample of vesicles and immediate NMR analysis showed an average of 90% reduction in channel activity over three runs. This behavior was also observed with **10** confirming inhibition of sodium transport in both cases. The result may be due to cation/cation repulsion, although it could also be explained by lack of incorporation of the oxidized channel into the membrane.

4. Cation flux using black lipid membrane preparations

Black lipid membrane recordings indicated that **9** was functioning as an ion channel (Fig. 8a).Voltage steps (10–20 mV increments) from −80 to +80 mV across the bilayer revealed single (and multiple) channel open level transitions varying in duration up to ~200 ms (Fig. 8a) with a mean single channel conductance of ~50–55 pS as shown in the amplitude histogram (Fig. 8b). Through assessment of the current–voltage relationship for amplitudes of the single channel events (Fig. 8c), it was evident that **9** behaved as an ohmic resistor in that the conductance did not change appreciably with varying membrane potentials. By contrast the frequency of opening of the channels was voltage-dependent in that the probability of channel open events (*Popen*) was markedly enhanced with increasing magnitude of the membrane potential (Fig. 8d). However, it was noted that this voltage-dependence was independent of the polarity of the potential increase. This finding may indicate that when the bilayer is more polarised, the channels assumed the appropriate orientation in the membrane in order to sustain an ion flux (regardless of the polarity as may be expected for a symmetrical ion channel).

After addressing the conductance and gating of **9**, we then recorded activity in an asymmetric gradient of 1M NaCl : 1M KCl in order to explore ion selectivity of the channel. Under these conditions on occasion (3 of 11 trials) the reversal potential (E_{rev}) shifted to ~ −15 to −20 mV compared to the E_{rev} = 0 mV when recorded in symmetrical conditions (Fig. 9, and Fig. 8a,b). Using the Goldman–Hodgkin–Katz equation, the relative permeabilities (P_{Na}/P_K) were calculated. Assuming that the channels were impermeable to chloride, it was determined that **9** has a 2–3-fold selective permeability for Na^+ over K^+. This finding is particularly important since equivalent measurements for the previously reported channel[17] showed that **10** demonstrated no selective permeability for either Na^+ or K^+ ions (not shown). Indeed, the activity of **10** in 1M NaCl: 1M KCl asymmetrical conditions showed E_{rev} ~ 0 mV indicating that this channel was

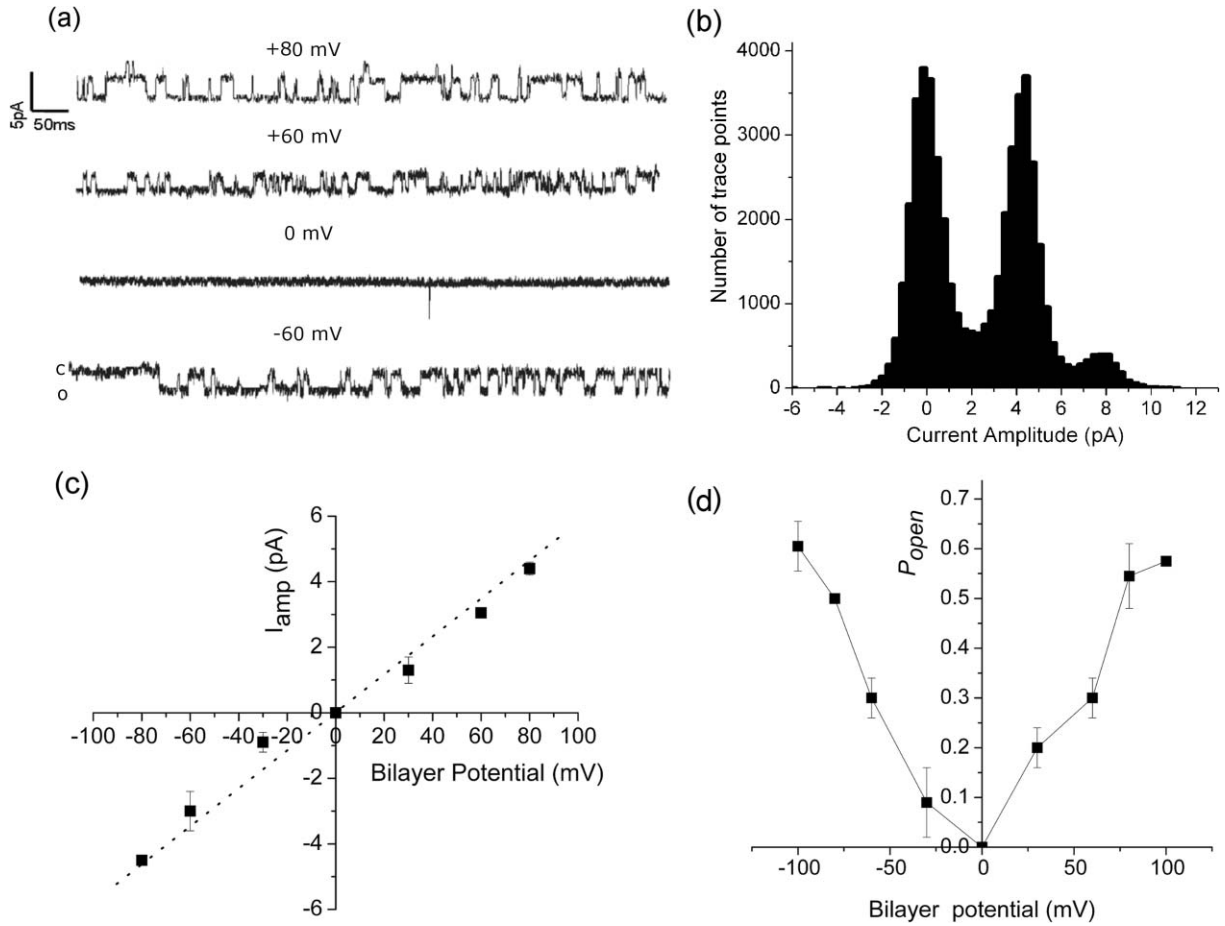

Fig. 8 **(a)** Typical planar bilayer traces for **9** for membrane held at ±80 mV and recorded in symmetrical 150 mM NaCl conditions. Note there were at least two channels incorporated in this membrane with closed times indicated by the '*C*", transitions to one channel open by 'O_1' and transitions to two channels open simultaneously by 'O_2'. **(b)** For the trace in (a) held at 80 mV, all points for 10 s of recording are plotted against current in an amplitude histogram. Note that at least two channels were active in this recording with single channel conductances of ~50 pS. **(c)** Using symmetrical conditions, the single channel current amplitudes (I_{amp}) are plotted against the holding potential for the bilayer (mV). Error bars indicate the range (max–min) of amplitudes recorded at a given potential for at least two independent recordings. A line of best fit (dotted) is superimposed on the plot indicating that the channels are essentially ohmic, with a conductance of ~50–55 pS. **(d)** The probability of opening (P_{open}) was calculated and plotted against the holding potential of the bilayer. Error bars indicate the range (max–min) of P_{open} values recorded at a given potential for at least two independent recordings. Note how the probability of open channel activity is markedly enhanced with increased potential regardless of polarity.

non-selective for the flux of monovalent cations. Inspection shows that **9** differs from **10** due to the replacement of the inner diaza-18 crown-6 rings of **10** by diaza-15-crown-5 units. Thus, the constriction in the inner rings of the channel may confer a level of ion selectivity for Na^+ over a K^+ flux. However, there was inconsistency in this selectivity result since in 8 of 11 recordings, the activity in asymmetrical conditions reversed at 0 mV, indicating no cation selectivity. Furthermore, single channel conductances recorded in symmetrical 150 mM KCl or LiCl were simliar (~50 pS) to those recorded in NaCl (data not shown). The lack of consistent selective behaviour suggests that the channel may adopt different conformations within the bilayer. Clearly the 18-crown-6 and 15-crown-5 rings need to align for the ions to pass through both and hence show selectivity. An alternative conformation, however, may involve the ferrocene nucleus lying perpendicular, rather than parallel, to the bilayer thus enabling the 15-crown-5 rings to act as a "relay" (see ref. 13), rather than a "filter", by rotation about the cpd–Fe bond. This would probably not afford selectivity between Na^+ and K^+ since the effect of ring size would be minimal. Clearly therefore, the molecular architecture described here does not afford consistent selectivity but may, at least, point a way forward.

Finally, to investigate gating by the redox-active ferrocene unit, we recorded channel activity of **9** and introduced the oxidizing agent, ceric (IV) ammonium nitrate (1 mM), at a concentration that was determined to have no effect on bilayer integrity in the absence of ion channel. Upon introduction of the oxidizing agent to both recording chambers, ion channel activity was consistently abolished (Fig. 10).

This activity was not restored through subsequent addition of a 6-fold excess of the reducing agent, sodium thiosulfate, possibly due to the size of the thiosulfate ion hindering the access to the ferrocene unit in the membrane. These data suggest that channel activity is markedly affected by the redox state. However, whether oxidation affects channel incorporation into the membrane, the configuration of **9** in the bilayer or blocks flux

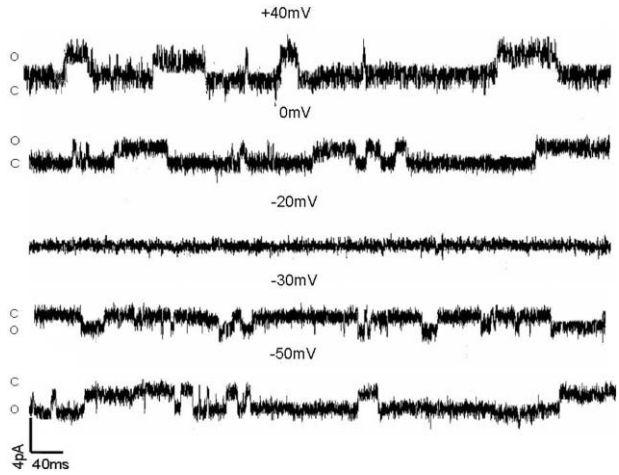

Fig. 9 Ion channel **9** is selectively permeable to Na^+ ions. The above traces were recorded in an asymmetrical gradient with 1 M NaCl in the *cis* chamber and 1 M KCl in the *trans.* The applied voltages are indicated above each trace with '*C*' indicating closed states and '*O*' open states. Note that at 0 mV channel openings were clearly evident while at –20 mV there was no measurable activity, indicating that the E_{rev} under these conditions shifted to between 0 to –20 mV compared to recordings using a symmetrical gradient (see Fig. 8a). The above recording was 1 of 3 (from 11 recordings in total) where activity was clearly evident at 0 mV in asymmetrical Na^+ : K^+ conditions.

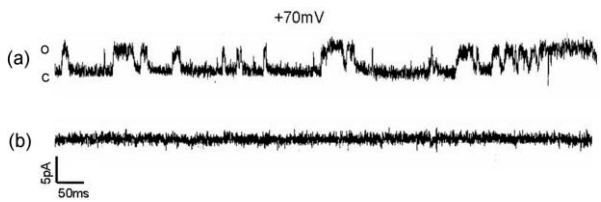

Fig. 10 Channel activity of (a) +70 mV and (b) +70 mV in the presence of a Ce^{4+} ion.

through irreversible oxidation of the ferrocene unit, remains to be determined.

Experimental

Melting points were determined on a hot-stage apparatus and are uncorrected. NMR spectra were recorded in $CDCl_3$ with TMS as the internal standard for ^1H (300 MHz) or $CDCl_3$ as the internal standard on a Varian Mercury 300 for ^{13}C (75 MHz). MALDI mass spectra were recorded on Bruker Reflex II TOF mass spectrometer retrofitted with Delayed Extraction at the Department of Chemistry, University of Florida in Gainesville, Florida, USA. All reactions were carried out under an atmosphere of nitrogen. Column chromatography was performed with A950–500 neutral alumina (60–325 mesh).

Thin layer chromatographic (TLC) analyses used aluminium oxide 60 F254 neutral on aluminium sheets with a 0.2 mm layer thickness (Merck) with 5% $MeOH/CH_2Cl_2$ as eluent. Chromatography columns were packed with alumina [neutral, type 507C, Fluka (0.05–0.15 mm; pH 7.0 ± 0.5)], or silica gel 60 (F254, 0.035–0.070 mm, Merck). Solvents were purified by standard procedures and were stored under nitrogen over molecular sieves (4–8 mesh). All the metal trifluoromethanesulfonates (triflates) except $Ca(SO_3CF_3)_2$ were used as obtained from Aldrich. Calcium trifluoromethanesulfonate was prepared as reported previously.[17]

Fluorescence methods

Fluorescence spectra were recorded using a Fluoromax 3 spectrofluorometer (Horiba Jobin Yvon). The fluorescence intensities of the ligands (1×10^{-5} M) excited at 363 nm were measured in acetonitrile at room temperature. Titrations were conducted by progressively adding the metal salts, injected as concentrated solutions, to a cuvette containing the ligand solution (2.5 ml). Samples were shaken briefly prior to each recording and the added equivalents of cation were plotted against the emission-intensity change in the 414–421 nm region.

Preparation of unilamellar vesicles from egg phosphatidyl choline by detergent dialysis

Unilamellar vesicles were prepared from egg yolk phosphatidylcholine using a modified detergent dialysis technique.[25] A sample of grade 1 lecithin (50 mg) in chloroform–methanol (Lipid Products, Redhill, Surrey, UK) was evaporated under N_2 and then dissolved in a solution (3 ml) containing 200 mM NaCl, 5 mM MES (pH: 6.5) and 300 mM, n-octyl-β-D-glucopyranoside (Calbiochem). The lipid solution was pipetted into a 6 mm diameter cellulose membrane dialysis tubing, and dialysed against 2.5 l of the external solution containing 200 mM NaCl, 5 mM MES (pH: 6.5) at room temperature. External solutions were pre-equilibrated and continually bubbled with N_2 throughout dialysis, and were changed every 10–12 h with three solution exchanges. In a final 8 h dialysis, the external solution was exchanged for 2.5 l of a deoxygenated solution containing 100 mM NaCl, 20 mM Na-tripolyphosphate, 50 mM choline chloride and 5 mM MES (pH: 6.5). The vesicle suspension was then carefully pipetted out of the dialysis bag and used immediately.

^{23}Na NMR measurements

Sodium cation flux was measured following the ^{23}Na NMR method of Riddell *et al*.[19] Sodium NMR spectroscopic measurements were performed on a JEOL Eclipse 400 NMR spectrometer with sodium observation at 105 MHz. A 5 mm tunable probe was used with the following acquisition parameters: tip angle 57°; sweep width ±11000 Hz; relaxation delay = 0.5 s; number of spectral points = 4 K; locked mode (D_2O). Each spectrum represents a collection of 200 scans Fourier transformed with an exponential line broadening of 0.2 Hz. NMR samples were prepared by mixing 675 μl of vesicular suspension, 75 μl of 100 mM NaCl/20 mM $Na_5P_3O_{10}$ in D_2O and 3.0 μl of 1 M $DyCl_3$ to obtain a sodium spectrum consisting of the intravesicular resonance separated from the extravesicular resonance by at least 6 ppm. All spectra were recorded at 291 K. Relaxation times (T_1) for the sodium signals were measured to be ~0.035 s. Linewidth measurements were obtained by deconvolution of the Na^+ resonance signals by a JEOL Lorentzian bandshape fit.

Ion channel recordings: black lipid membrane experiments

Standard black lipid membrane techniques were employed to record synthetic ion channel activity in planar lipid bilayers

with phospholipid membranes formed through a painted bilayer method.[25] Phosphatidylcholine (DOPC) and phosphatidylglycerol (DOPG, Avanti Polar Lipids, Birmingham, AL, USA) were stored as chloroform dispersions at –80 °C in sealed glass vials. Channel **9** was stored in methanol at –80 °C prior to use. Electrolyte solutions in distilled water consisted of (i) for symmetrical solutions: 150 mM NaCl, (ii) for asymmetrical solutions, 1 M NaCl/1M KCl, with 10 mM HEPES, titrated to pH 7.2 with NaOH or KOH and stored at 4 °C. A lipid/ion channel solution, 85:15% DOPC/DOPG including 0.5–1 μg of **9**/mg of lipid, was prepared by evaporating off the chloroform/methanol from the stock solutions under a stream of nitrogen, before dispersal in n-decane (50 mg/ml lipid). This lipid/ion channel solution was used to pre-treat the aperture in a delrin bilayer cup. The dispersion was spread using a 'painting stick' fashioned from a glass Pasteur pipette. The stick was dipped in the decane solution and a small quantity painted across the 200 μm-diameter hole in the cup and allowed to dry. The electrolyte solutions were added to the delrin cup (referred to as *cis*, volume 3 ml) and to the block chamber (*trans*, volume 3 ml). Silver-silver chloride electrodes linked the electrometer head to the cell *via* agar bridges (2% agar in 3 M KCl) with the reference electrode placed in the *cis* chamber. Electrodes were stored in bleach and the bridges were stored at 4 °C in 3 M KCl. The whole apparatus was enclosed in a grounded Faraday cage positioned on a metal base plate resting on an air-cushioned table (Warner Instrument Corporation, Hamden, CT).

To form a bilayer, the painting stick was again dipped in the lipid/decane solution, and the stick was submerged in the electrolyte solution and drawn across the aperture in the cup. Lipid bilayer formation through thinning usually occurred within 1–10 min resulting in a final capacitance of the bilayers ~80–120 pF. Currents were recorded using a Warner amplifier (model BC-525D) using variable holding potentials, filtered at 1 kHz with a low-pass 8-pole Bessel filter (Model LPF-8, Warner Instruments) and then acquired using Clampex 9.2 software (Axon Instruments) with a sampling rate of 4 kHz. In experiments involving the oxidizing agent, 1 mM ammonium cerium (IV) nitrate was added to both chambers and the solutions were stirred using a magnetic stirrer. This concentration of the oxidizing agent was determined not to disrupt the integrity of the membrane bilayers. All experiments were carried out at room temperature.

Synthesis of ion channel

4,13-Diaza-18-crown-6 was purchased from IBC Advanced Technologies, Inc. N-*t*-Butoxycarbonyl-diaza-18-crown-6 (**1**), N-*t*-butoxycarbonyl-diaza-15-crown-5 (**5**), N-(9-anthrylmethyl)-N′-*t*-butoxycarbonyl-diaza-18-crown-6 (**2**), N-(9-anthrylmethyl)-diaza-18-crown-6 (**3**), and N-(9-anthrylmethyl)-N′-(10-bromodecyl)diaza-18-crown-6 (**4**) were all prepared as described previously.[17]

N-(9-Anthrylmethyl)-N′[10-(N′-t-butoxycarbonyl-diaza-15-crown-5)decyl]-diaza-18-crown-6 (6). A solution of N-(9-anthrylmethyl)-N′-(10-bromodecyl)-diaza-18-crown-6 (**4**, 0.11 g 0.16 mM) and N-*t*-butoxycarbonyl-diaza-15-crown-5 (**5**, 0.05 g 0.16 mmol) in propionitrile (2 ml) was heated under reflux over anhydrous Na_2CO_3 (0.33 g, 3.19 mM) and KI (3 mg, 0.02 mM) for 20 h under nitrogen. The mixture was cooled, filtered and concentrated *in vacuo*. The yellow residue was redissolved in CH_2Cl_2 (5 ml), washed with water (10% w/v, 3 × 5 ml), dried ($MgSO_4$) and concentrated *in vacuo*. The residue was purified by column chromatography (alumina, MeOH/CH_2Cl_2) to give **6** as an orange oil (0.10 g, 63%). ^{1}H NMR ($CDCl_3$) δ 8.53 (d, J = 8.7 Hz, 2H), 8.40 (s, 1H), 8.0 (d, J = 8.5 Hz, 2H), 7.53–7.43 (m, 4H), 4.56 (s, 2H), 3.84–3.75 (m, 4H), 3.74–3.30 (m, 28H), 3.31–3.12 (m, 4H), 3.11–2.80 (m, 10H), 2.71–2.48 (m, 2H), 1.75–1.40 (m, 13H), 1.39–1.18 (12H); ^{13}C NMR ($CDCl_3$) δ 155.1, 131.3, 131.3, 130.2, 128.9, 127.4, 125.5, 125.1, 124.7, 79.5, 70.8, 70.5, 70.3, 70.2, 70.0, 69.8, 69.4, 69.2, 67.9, 67.4, 55.8, 54.8, 53.8, 53.4, 52.8, 52.6, 51.6, 49.2, 49.0, 48.8, 29.4, 29.2, 28.4, 27.2, 27.1. HRMS (MALDI-TOF): m/z calculated for $C_{52}H_{84}N_4O_9$ [M – $C_{15}H_{10}$ + H]$^+$ 719.5529, found 719.5629; [M – $C_{15}H_{10}$ + Na]$^+$ calculated 741.5348, found 741.5453.

N-(9-Anthrylmethyl)-N′-[10-(diaza-18-crown-6)decyl]-diaza-15-crown-5 (7). N-(9-Anthrylmethyl)-N′[10-(N′-t-butoxycarbonyl-diaza-15-crown-5)decyl]-diaza-18-crown-6 (**6**, 0.09 g, 0.10 mM) was dissolved in a mixture of TFA (0.35 g, 3.09 mM) and CH_2Cl_2 (1 ml) and stirred at 20 °C for 16 h. The solution was evaporated to dryness and the residue was dissolved in CH_2Cl_2 (3 ml), washed with Na_2CO_3 solution (10% w/v, 3 × 3 ml), dried ($MgSO_4$) and concentrated *in vacuo* to give **7** as an orange oil (77 mg, 96%). ^{1}H NMR ($CDCl_3$) δ 8.46 (d, J = 8.8 Hz, 2H), 8.31 (s, 1H), 7.90 (d, J = 8.5 Hz, 2H), 7.45–7.33 (m, 4H), 4.50 (s, 2H), 3.58–3.45 (m, 28H), 2.82 (t, J = 5.7 Hz, 4H), 2.71–2.61 (m, 12H), 2.39 (t, J = 7.7 Hz, 4H), 1.35 (brq, 4H), 1.28–1.06 (pseudo-s, 12H); ^{13}C NMR ($CDCl_3$) δ 131.3, 131.3, 130.4, 128.8, 127.3, 125.5, 125.2, 124.7, 70.7, 70.5, 70.2, 70.1, 70.0, 69.9, 69.2, 56.6, 56.0, 54.4, 54.3, 53.9, 53.7, 51.8, 48.9, 48.7, 29.5, 27.4, 27.0, 26.9. 809. HRMS (MALDI-TOF): m/z calculated for $C_{47}H_{76}N_4O_7$ [M + H]$^+$ 809.5787, Found: 809.5882; calculated [M + Na]$^+$ 831.5606, found 831.5720.

1,1′-Ferrocenedicarboxylic acid was prepared as described previously.[26]

1,1′-Bis-(chlorocarbonyl)ferrocene (8). Oxalyl chloride (8.13 g, 64.08 mM) was added over 1 min to a suspension of 1,1′-ferrocenedicarboxylic acid (2.11 g, 7.70 mM) in dry CH_2Cl_2 (37 ml) under nitrogen. The mixture was heated under reflux for 9 h and stirred at 20 °C for a further 1.5 h. The solution was concentrated *in vacuo* and the residue recrystallized from n-pentane to give **8** as red crystals (1.90 g, 79%), m.p.= 106.0–109.0 °C, ^{1}H NMR ($CDCl_3$) δ 5.05 (t, J = 2.0, 4H), 4.77 (t, J = 2.0 Hz, 4H); ^{13}C NMR ($CDCl_3$) δ 168.7, 77.3, 76.1, 74.1.

1,1′-Bis-[N-carbonyl-N′-[-10-(N′-(9-anthrylmethyl)-diaza-18-crown-6)decyl]-diaza-15-crown-5]ferrocene (9). 1,1′-Bis(chlorocarbonyl)ferrocene (**8**, 22 mg, 0.07 mM) in dry toluene (2.67 ml) was added dropwise over 5 min to a solution of N-(9-anthrylmethyl)-N′-[10-(diaza-18-crown-6)decyl]-diaza-18-crown-6 (**7**, 0.11 g, 0.14 mM) and dry Et_3N (14 mg, 0.14 mM) in dry toluene (2.67 ml). The mixture was stirred at 20 °C for 24 h under nitrogen, filtered and concentrated *in vacuo* to give an orange residue. The product **9** was obtained by column chromatography (alumina, 4–5% MeOH/ethyl acetate) as an orange oil (0.12 g, 86%). ^{1}H NMR ($CDCl_3$) δ 8.54 (d, J = 8.5 Hz, 4H), 8.40 (s, 2H), 7.99 (d, J = 8.0 Hz, 4H), 7.54–7.41 (m, 8H), 4.73–4.66 (m, 4H), 4.58 (s, 4H), 4.48–4.46 (m, 4H), 3.80–3.40 (m, 64H), 3.10–2.85 (m, 8H), 2.84–2.56 (m, 16H), 2.52–2.45 (m 8H),

1.64–1.37 (m, 8H), 1.36–1.05 (pseudo-s, 24H); ^{13}C NMR ($CDCl_3$) δ 172.1, 131.3, 131.3, 130.3, 128.9, 127.4, 125.5, 125.1, 124.7, 77.2, 71.9, 71.8, 70.6, 70.4, 70.0, 53.8, 53.4, 51.7, 29.6, 29.5, 29.4, 27.4, 27.3. HRMS (MALDI-TOF): *m/z* calculated for $C_{106}H_{158}FeN_8O_{16}$ $[M + H]^+$ 1857.1252, Found: 1857.1288, calculated $[M + Na]^+$ 1879.1071, found 1879.1356.

Conclusions

Spectroscopic and cyclic voltammetry studies suggest that the synthetic, redox-active ion channel **9** coordinates cations to afford a 'billiard ball' mechanism of ion transport analogous to that found with natural protein channels. This study has also shown that **9** conducts Na^+ ions through lipid bilayers at a rate that is approximately five times faster than the ionophore, monensin. Although the data were inconsistent, **9** also demonstrated some selectivity for supporting a Na^+ flux over a K^+ flux, possibly dependent on the appropriate orientation of the channel in the membrane. Oxidation of the ferrocene unit within the channel inhibits the ion transport, demonstrating the potential role of a redox-active center as a switch in regulating transmembrane cation flux.

Acknowledgements

We would like to acknowledge: Dr Charles Amass, Chemistry Department, Smith College for helpful advice on the sodium NMR spectroscopy, the National Science Foundation (NSF grant# CHE-0513445), and Merck/AAAs Undergraduate Science Research program for supporting the work of all the undergraduates coauthors (Nylander, Wardlaw, Gibson, Valentine, Onyewadume, Ahove, Woodbury and Mongare) and undergraduates: Angela Saquibal, Mary Banks, Anu Maharjan, Monica Wang and Jill Flynn.

Notes and references

1 D. J. Aidley and P. R. Stanfield, *Ion channels : molecules in action*, University Press, Cambridge, 1996.
2 W. D. Stein, *Channels, Carriers and Pumps*, Academic Press, New York, 1990.
3 (*a*) T. M. Fyles, *Chem. Soc. Rev.*, 2007, **36**, 335; (*b*) G. W. Gokel and I. A. Carasel, *Chem. Soc. Rev.*, 2007, **36**, 378; (*c*) U. Koert and P. Reiss, *Supramol. Chem.*, 2002, **2**, 29; (*d*) G. W. Gokel and A. Mukhopadhyay, *Chem. Soc. Rev.*, 2001, **30**, 274.
4 (*a*) F. Otis, N. Voyer, A. Polidori and B. Pucci, *New J. Chem.*, 2006, **30**, 185; (*b*) G. G. Kochendoerfer, D. Clayton and C. Becker, *Protein Pept. Lett.*, 2005, **12**, 737; (*c*) E. Biron, F. Otis, J.-C. Meillon, M. Robitaille, J. Lamothe, P. Van Hove, M.-E. Cormier and N. Voyer, *Bioorg. Med. Chem.*, 2004, **12**, 1279; (*d*) G. W. Gokel, P. H. Schlesinger, N. K. Djedovic, R. Ferdani, E. C. Harder, J. Hu, W. M. Leevy, J. Pajewska, R. Pajewski and M. E. Weber, *Bioorg. Med. Chem.*, 2004, **12**, 1291; (*e*) J.-C. Meillon and N. Voyer, *Angew. Chem., Int. Ed. Engl.*, 1997, **36**, 967.
5 (*a*) D. T. Bong, T. D. Clark, J. R. Granja and M. R. Ghadiri, *Angew. Chem., Int. Ed.*, 2001, **40**, 988; (*b*) M. Amorin, L. Castedo and J. R. Granja, *Chem. Eur. J.*, 2008, **14**, 2100; (*c*) S. Fernandez-Lopez, H. S. Kim, E. C. Choi, M. Delgado, J. R. Granja, A. Khasanov, K. Kraehenbuehl, G. Long, D. A. Weinberger, K. M. Wilcoxen and M. R. Ghadiri, *Nature*, 2001, **412**, 452.
6 N. Sakai and S. Matile, *Angew. Chem., Int. Ed.*, 2008, **47**, 9603.
7 Y. J. Jeon, H. Kim, S. Jon, N. Selvapalam, D. H. Oh, I. Seo, C. S. Park, S. R. Jung, D. S. Koh and K. Kim, *J. Am. Chem. Soc.*, 2004, **126**, 15944.
8 M. E. Weber, W. Wang, S. E. Steinhardt, M. R. Gokel, W. M. Leevy and G. W. Gokel, *New J. Chem.*, 2006, **30**, 177.
9 W. Wang, C. R. Yamnitz and G. W. Gokel, *Heterocycles*, 2007, **73**, 825.
10 J. Carlos Iglesias-Sanchez, W. Wang, R. Ferdani, P. Prados, J. de Mendoza and G. W. Gokel, *New J. Chem.*, 2008, **32**, 878.
11 G. W. Gokel and M. M. Daschbach, *Coord. Chem. Rev.*, 2008, **252**, 886.
12 W. Wang, R. Li and G. W. Gokel, *Chem. Commun.*, 2009, 911.
13 C. L. Murray, H. Shabany and G. W. Gokel, *Chem. Commun.*, 2000, 2371.
14 (*a*) D. A. Dougherty and H. Lester, *Angew. Chem., Int. Ed.*, 1998, **37**, 2329; (*b*) P. J. Cragg, M. C. Allen and J. W. Steed, *Chem. Commun.*, 1999, 553 .
15 P. Schmitt, P. D. Beer, M. G. B. Drew and P. Sheen, *Angew. Chem., Int. Ed. Engl.*, 1997, **35**, 1840.
16 H. Shabany, C. L. Murray, C. A. Gloeckner, M. A. Grayson, M. L. Gross and G. W. Gokel, *Chem. Commun.*, 2000, 2375.
17 A. C. Hall, C. Suarez, A. Hom-Choudhury, A. N. A. Manu, C. Dennis Hall, G. J. Kirkovits and I. Ghiriviga, *Org. Biomol. Chem.*, 2003, **1**, 2973.
18 M. M. Pike, S. R. Simon, J. A. Balshi and C. S. Springer, *Proc. Natl. Acad. Sci. U. S. A.*, 1982, **79**, 810.
19 (*a*) F. G. Riddell and M. K. Hayer, *Biochim. Biophys. Acta*, 1985, **817**, 313; (*b*) F. G. Riddell and S. J. Tompsett, *Biochim. Biophys. Acta*, 1990, **1024**, 193; (*c*) D. Duval, F. G. Riddell, S. Rebuffat, N. Platzer and B. Bodo, *Biochim. Biophys. Acta*, 1998, **1372**, 370.
20 G. R. A. Hunt and J. A. Veiro, *Biochem. Soc. Trans.*, 1986, **14**, 602.
21 K. Ashwani, S. Mogeswaran and O. Sutherland, *Tetrahedron*, 1986, **42**, 3291.
22 (*a*) A. P. de Silva and S. A. de Silva, *J. Chem. Soc., Chem. Commun.*, 1986, 1709; (*b*) K. Kubo, R. Ishige and T. Sakurai, *Talanta*, 1999, **49**, 339.
23 C. Hamamci, H. Hoşgören and S. Erdoğan, *Talanta*, 1998, **47**, 229.
24 E. K. Elliott, M. M. Daschbach and G. W. Gokel, *Chem. Eur. J.*, 2008, **14**(19), 5871.
25 A. J. Williams, in *Microelectrode Techniques–The Plymouth Workshop Handbook*, ed. D. Ogden, The Company of Biologists Ltd., Cambridge, 2nd edn, 1994, pp. 79–101.
26 V. G. Albano, L. Busetto, F. Marchetti, M. Monari, S. Zacchini and V. Zanotti, *J. Organomet. Chem.*, 2005, **690**, 4666.

